ICAS-80-11.3

FLOW COMPUTATION AROUND MULTI-ELEMENT AIRFOILS IN VISCOUS TRANSONIC FLOW

H. Rosch and K.D. Klevenhusen
VFW GmbH, Bremen, FRG

ABSTRACT

A new singularity method is applied to multi-element airfoils in the physical plane for calculating both, the incompressible velocities and the incompressible potential- and streamfunction along the contur of each element. The values of the preceding computation are used to build an orthogonal grid in which the airfoil is mapped to a line in the streamline plane. The computational domain is this streamline plane wherein the full transonic potential equation is solved using a finite difference method. The geat influence of viscous effects has been incorporated using the so-called surface transpiration concept. The representation of the displacement effect of the boundary layer and wakes is based on the well-known integral method and a trailing edge flow concept, which includes normal pressure gradients and wake curvature effects. Comparisons of the theory with high Reynolds number experiments show the good agreement for pressure distribution and lift.

NOMENCLATURE

a	Local Speed of Sound
B	Square of the compressible velocities
C	Chord length
C_p	Pressure coefficient
M_∞	Mach number at infinity
n	Normal direction
Q	Square of the incompressible velocities
q	Flow speed
s	Arc length along airfoil and wake streamline
t	Tangential direction
u,v	Velocity components
x,y	Cartesian coordinates
x',y'	"disturbance" coordinates
α	Angle of attack
β	Prandtl -factor $\sqrt{1-M_\infty^2}$
γ	Specific heats
δ^*	Displacement thickness
Θ	Momentum thickness
$\varkappa$	Curvature $\left(\frac{1}{u}\frac{\partial u}{\partial n}\right)$
ϱ	Density
Φ	Compressible potentialfunction
φ	Incompressible potentialfunction
ψ	Incompressible streamfunction
$\Delta\varphi$	Potential jump at the trailing edge

Subscripts

A	Airfoil
n	Direction normal to airfoil and wake
SEP	Separation point
TE	Trailing edge
t	Direction tangent to wake
w	Wake
x	Derivative in x-direction
y	Derivative in y-direction
δ	Denotes boundary layer edge
φ	Derivative in φ-direction
ψ	Derivative in ψ-direction
υ	Iteration count
∞	Free Stream

I. Introduction

Several published methods are known for the solution of two-dimensional viscous, steady transonic flow problems. These methods can generally be divided into two types. The first uses the small disturbance transonic potential equation [1,2] and added a boundary layer code to include viscous effects.

The second method, and the one on which the work presented here is based, uses the full transonic potential equation in connection with various boundary layer codes [3,4,5,6,7] . They all solve the equation in a curvilinear coordinate system provided by conformal mapping based on an early work by Sells [8] .

The present work solves the transonic potential equation by a finite difference method using an orthogonal bodyfitted streamline coordinate system. This provides a transonic computational plane where one set of mesh lines is approximately aligned with the flow and the other is normal to the boundaries of the flow. The transformed coordinates used are the incompressible stream function and potential function, which are obtained

from an incompressible solution of the flow field in question.

An early paper of Colehour [9] uses a similar approach but unlike the present paper he solves the incompressible stream function equation $\nabla^2\psi=0$ using a finite difference method to get the desired stream function and potential function. The present method uses a new singularity distribution which is applied to bodies or even multi-element airfoils in the physical plane calculating both the incompressible velocities and the stream function and potential function along the surface of each element.

In calculating the boundary layer development, a laminar boundary layer is assumed to commence from the stagnation point and to continue to some specified transition position is reached where a turbulent boundary layer is initiated. The representation of the displacement effect of boundary layers and wakes is developed by Thiede et al [10] and is based on the well-know integral method, see for details [11] , expanded to handle the wake displacement effects too.

An iterative procedure is employed to obtain consistent solutions for the inviscid flow and the boundary layer. In the interaction procedure the concept of the surface transpiration model of Lock [12] is used to represent the effect of the various viscous layers on the outer potential flow. In this manner the repetition of the airfoil transformation after every boundary layer calculations is avoided. An allowance for curvature effects of the boundary layer and the wake is included in these boundary conditions.

The subsequent paper is devided into four parts. The first describes the formulation of the compressible flow equations with viscous effects, the second the representation of the boundary layer and wake the third the inviscid-viscous interaction scheme while in the fourth part some of the results are presented.

II. The basic inviscid method

The governing equation chosen for this analysis is the full inviscid equation for compressible flow. The usual form of this equation for two-dimensional flow is:

$$\left(a^2-\phi_x^2\right)\phi_{xx}-2\phi_x\phi_y\phi_{xy}+\left(a^2-\phi_y^2\right)\phi_{yy}=0 \qquad (1)$$

The local speed of sound can be determind from the energy equation

$$a^2+\frac{\gamma-1}{2}q^2=\left(\frac{1}{M_\infty^2}+\frac{\gamma-1}{2}\right)q_\infty^2 \qquad (2)$$

and on the profile the solution should satisfy the Neumann boundary condition

$$\frac{\partial\Phi}{\partial n}=0 \qquad (3)$$

Before the transonic solution is started, these equations are transformed to the incompressible $\varphi-\psi$-plane.

Consider for example an two-element airfoil given in cartesian coordinates, Fig. 1.

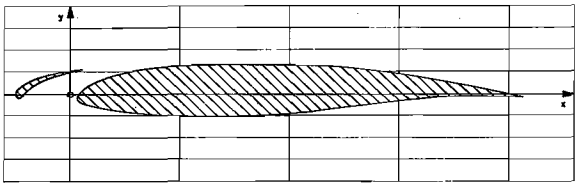

Fig. 1 Airfoil with slat in cartesian coordinates

For the determination of the incompressible flow around this especially airfoil a Dirichlet-problem has to be solved:

$$\nabla^2\psi=0 \qquad (4)$$

with

$$\psi=\text{const} \qquad (5)$$

at the boundaries of the airfoil and

$$\psi=\psi_\infty \qquad (6)$$

at infinity. Differing from the well-known panel methods, see for example [13,14] and only for numerical reasons a doublet distribution with tangential doublet axes along the contour is used. With this distribution arbitrary thick and infinite thin elements can be used without any difficulty.

The singularity model leads to a well behaved system of linear equations and is very appropriate for calculating the incompressible flow around multi-element airfoils. For further details one is referred to Klevenhusen [15] .

The streamline coordinate system necessitates the velocity potential distribution along the contours which is obtained by taking the same doublet strength as for the streamfunction but positioning the doublet axes normal to the contour. The behavior of the velocity potential of doublets is in such a way that the unavoidable numerical errors decreases with increasing distance from the locus of the doublet. Therefor a doublet model is more suitable than a source or vortex model for determining the potential and streamfunction. Only open contours and non-constant streamfunction on the boundary require additional singularity distributions.

The transformed transonic potential equation requires the knowledge of the squares of the incompressible velocities at every node point (φ, ψ) in the streamline plane. The velocities are considered as functions of φ and ψ . Furthermore we can define disturbance velocities

$$u' = u - U_\infty \cos\alpha \qquad (7)$$

$$v' = v - U_\infty \sin\alpha \qquad (8)$$

The velocities u' and v' are potential functions in the $\varphi - \psi$-plane and bounded at infinity. To get the required velocities at the node points a Laplace equation in the flow field

$$u_{\varphi\varphi} + u_{\psi\psi} = 0 \qquad (9)$$

is to be solved. The necessary boundary conditions are known from the calculation in the physical plane. A similar Laplace equation can be formulated for v' in the same way.

These two boundary value problems can be solved by doublet distributions along the slit with oblique doublet axes in the streamline plane using the above mentioned panel method. After solving the boundary value problems the doublet distributions are known and the velocities u and v can be calculated at every given point in the streamline plane.

Finially the physical coordinates are also conjugate harmonic functions in the streamline plane. Defining "disturbance coordinates"

$$x' = x - \varphi\cos\alpha + \psi\sin\alpha \qquad (10)$$

$$y' = y - \varphi\sin\alpha + \psi\cos\alpha \qquad (11)$$

the x' and y' are bounded at infinity so we can handle x' and y' in the same way as u' and v'. An example of this procedure is given in Fig. 2.

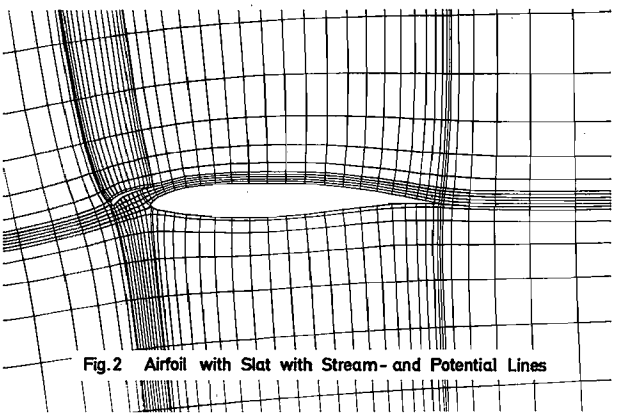

Fig.2 Airfoil with Slat with Stream- and Potential Lines

The computational domain is the streamline plane, Fig. 3 wherein the full transonic potential equation is solved using a finite difference method. The transonic potential

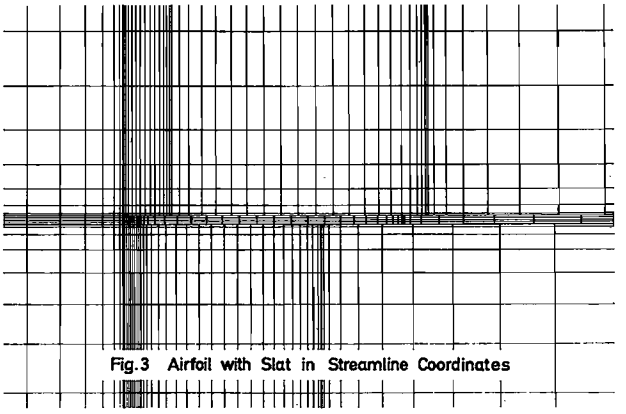

Fig.3 Airfoil with Slat in Streamline Coordinates

equation (1) in the incompressible streamline coordinate system is given by

$$2a^2\left(\Phi_{\varphi\varphi} + \Phi_{\psi\psi}\right) - \left(\Phi_\varphi B_\varphi + \Phi_\psi B_\psi\right) = 0 \qquad (12)$$

with

$$B = \left(\Phi_\varphi^2 + \Phi_\psi^2\right)\cdot Q \qquad (13)$$

which denotes the square of the local compressible velocity and

$$Q = \varphi_x^2 + \varphi_y^2 \qquad (14)$$

which denotes the square of the local incompressible velocity. The equation of the speed of sound (2) is transformed to

$$a^2 = a_\infty^2 - \frac{\gamma-1}{2}(B - U_\infty^2) \qquad (15)$$

A good approximation for the compressible streamlines is achieved using the same angle of attack for the determination of the grid and for calculating the transonic flow. Since the mesh lines are approximately aligned with the flow the use of a rotated difference scheme is eliminated and the transonic potential equation (12) can be simplified considerably, as all first derivatives normal to the streamline are incremental and terms of second order can be neglected:

$$2a^2(\Phi_{\varphi\varphi} + \Phi_{\psi\psi}) = 2Q\Phi_\varphi^2\Phi_{\varphi\varphi} + \Phi_\varphi^2(\Phi_\varphi\Phi_\varphi + \Phi_\psi\Phi_\psi) \qquad (16)$$

All transonic calculations using the present method are based upon this equation. The boundary condition is given by

$$\Phi_\psi = 0 \qquad (17)$$

at the contour of each element.

III. Representation of the boundary layer

In the interaction procedure the concept of displacement thickness is used to represent the effect of the various viscous layers on the outer potential flow. Instead of adding the displacement thickness to the airfoil geometry, a distribution of sources along the airfoil surfaces and along the wake center lines is utilized for the simulation of the viscous flow displacement effects. In this case we may rewrite the boundary condition, eq (17), for the inviscid flow as follows:

$$\Phi_\psi = v_n/\sqrt{Q} \qquad (18)$$

where v_n is the normal outflow from the airfoil due to the boundary layer. The viscous boundary conditions are as follows:

- on the airfoil

$$v_{n_A} = \frac{1}{\varrho_\delta}\frac{d}{ds}(\varrho_\delta q_\delta \delta^*) \qquad (19)$$

- in the wake

$$\Delta v_{n_W} = \frac{1}{\varrho_\delta}\frac{d}{ds}(\varrho_\delta q_\delta \delta^*) \qquad (20)$$

$$\Delta v_{t_W} = -\varkappa q_\delta (\delta^* + \Theta) \qquad (21)$$

For details about the boundary layer codes one is referred to [10,11] .

A further change to the inviscid scheme is introduced in order to allow for the effect of the curvature of the airfoil and wake on the pressure change across the viscous layer and is given by

$$\Delta p_{A,W} = -\varkappa \varrho_\delta q_\delta^2 (\delta^* + \Theta) \qquad (22)$$

which must be added to the inviscid pressure distribution. The required curvature used in equations (21) and (22) is given by

$$\varkappa = \frac{1}{q}\frac{\partial q}{\partial n} \qquad (23)$$

which is positive in the wake. It is shown in Ref. 7 that equation (22) is approximately equivalent to adjust the alculated velocity q to q', where

$$q' = q\,[1 + \varkappa(\delta^* + \Theta)] \qquad (24)$$

with a similar correction for the velocity in the wake. The velocity q' is used to calculate the boundary layer.

IV. The numerical procedure

The mathematical formulations of the inviscid and viscous flow problems are coupled through their respective boundary conditions. The objective of the solution procedure is to find those particular distributions of surface velocity and boundary layer displacement thickness which simultaneously satisfy both the potential flow problem and the boundary layer problems.

A basic feature of the numerical scheme is that the repetition of the airfoil transformation after every boundary layer calculation is avoided. The numerical solution of the transonic boundary value problem proceeds in a manner similar to that of Murman and Cole [16] . A successive line overrelaxation method is used where the flow field is swept in the downstream direction only, and difference formulas are switched depending on whether the flow is subsonic or supersonic.

A solution is sought for the same angle of attack in both calculations, i.e. calculations to get the desired streamline plane and to get the desired transonic results. This assures the proper alignment of the incompressible streamlines with the compressible ones in the converged transonic solution.

During the iterative procedure, Fig. 4, a prescribed Number, NS1,

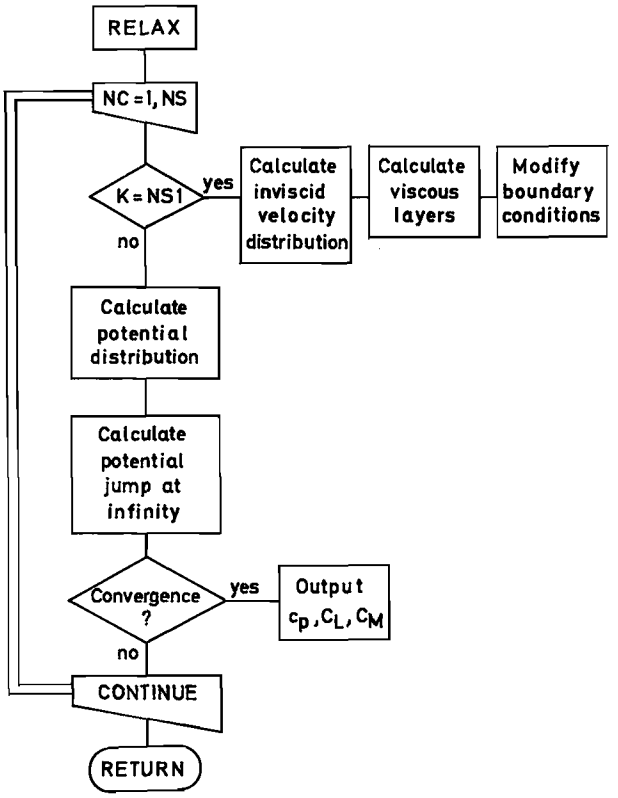

Fig. 4 Flow Chart for Iterative Methods

of the inviscid iterations is performed with the current boundary conditions. The velocity is then calculated on the airfoil surface and along the wake, and is used to calculate the current boundary layer. The boundary layer on each surface is calculated seperately and is extended beyond the trailing edge to obtain the part of the wake on either side of the trailing edge streamline. The pressure distribution is specified at node points along the dividing streamline in the streamline plane, but is specified for the boundary layer analysis as values at the corresponding x and y coordinate points, starting at the stagnation point rather than the leading edge and proceding downstream towards infinity an each surface.

As results the boundary layer calculations produces the displacement thickness, δ^*, and the momentum thickness, Θ, at the various meshpoints. Underrelaxation is employed in order to determine the actual values of the displacement thickness

$$\delta^*_\nu = \delta^*_{\nu-1} + \text{RDEL}\,(\delta^*_\nu - \delta^*_{\nu-1}) \qquad (25)$$

and the momentum thickness

$$\Theta_\nu = \Theta_{\nu-1} + \text{RDEL}\,(\Theta_\nu - \Theta_{\nu-1}) \qquad (26)$$

where RDEL is an underrelaxation parameter. With these relaxed values equations (19), (20), (21) and (24) are used to calculate the new boundary conditions and further flow field calculations are performed with the new boundary conditions.

After every NS1 inviscid iterations have been performed the whole cyle is repeated. This process continues until either a certain convergence criteria is satisfied or until a specified number of iterations have been completed. After the completation of the iterative procedure the lift coefficients on the airfoil are calculated.

V. Result

Several test cases have been selected to demonstrate the flexibility of the method. The first example shows pressure distributions about a two-dimensional airfoil section, the same as in Fig. 2. The calculations, Fig. 5, have been done for

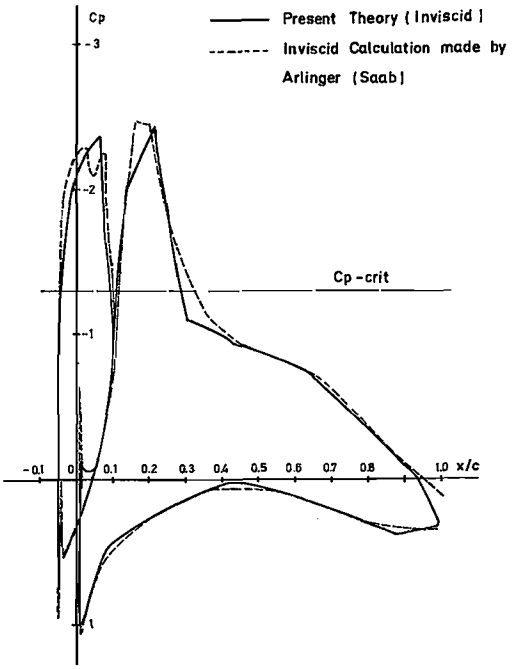

Fig.5: Two-Element Airfoil, $M_\infty = .6$, $\alpha = 6°$

the inviscid case. The agreement between the present result and the result obtained by Arlinger [17] are good, however Arlinger used a conformal mapping [18] to get the desired computational mesh.

The next two figures demonstrate the effect of the pressure variation across the viscous layer. Fig. 6 shows for an NACA 65_1-213 airfoil

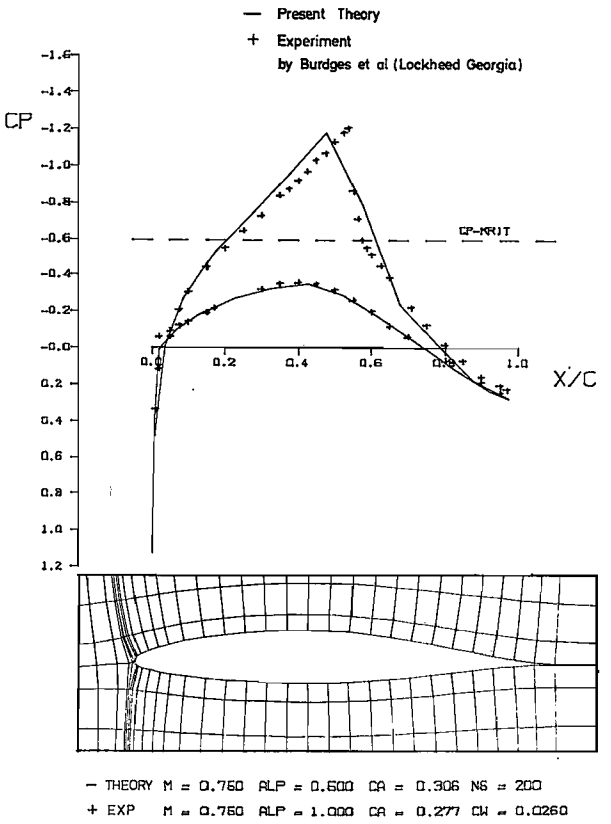

Fig.6: NACA 65.1-213, α = 0.5 Airfoil
Calculation without Curvature Effects

a calculation with a correction for viscous effects only on the profile and without the described normal pressure correction. Comparison is made with measurements obtained by Burdges et al [19]. The next figure, Fig 7, shows the including of the normal pressure correction. It clearly demonstrates the influence of the pressure correction on the last 10% of the airfoil chord. With this correction the agreement between theory and measurement for this simple airfoil shape is excellent.

Some typical results of a comparison of the pressure distributions for the supercritical airfoil VFW-VA2 are presented in the next two figures. Fig. 8 shows a calculation

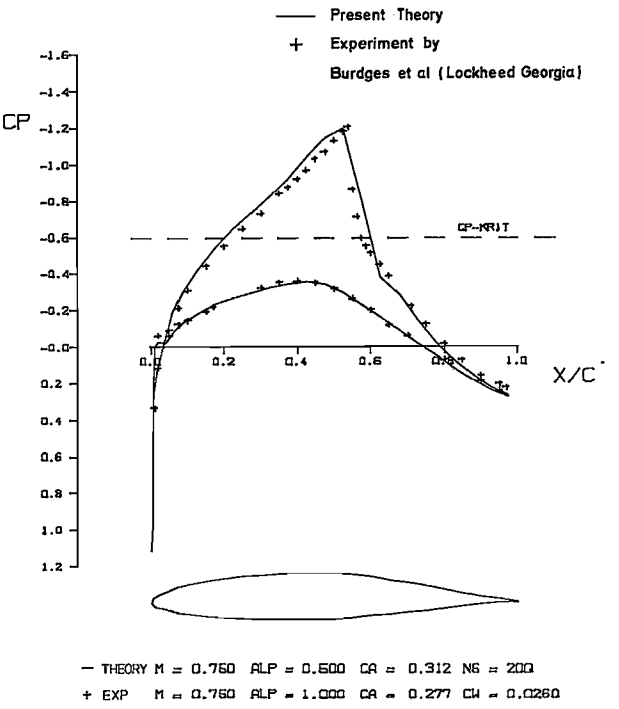

Fig. 7: NACA 65_1 - 213 α = .5 Airfoil
Calculation with Curvature Effects

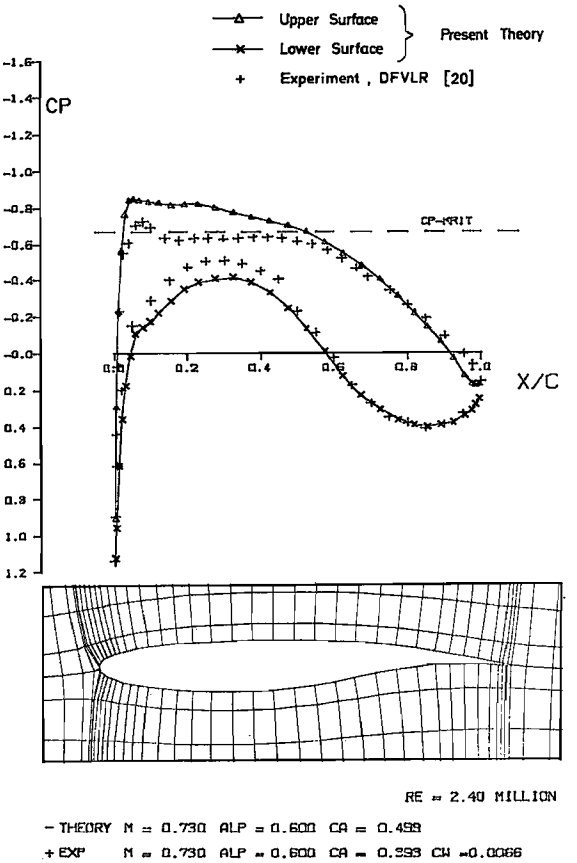

Fig.8: VFW VA-2 Airfoil
Calculation without Wake Effects

with the pressure correction but without the wake displacement effects. The experiment is taken from Ref. [20] . In the next calculation the effects of the wake are included and Fig. 9

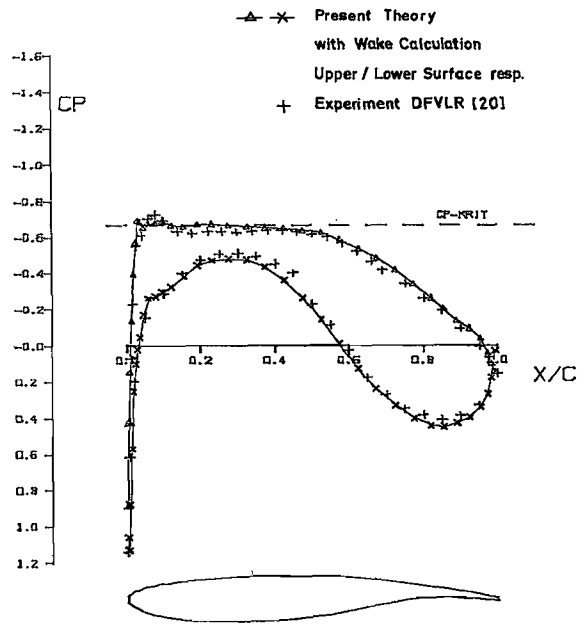

RE = 2.40 MILLION

– THEORY M = 0.730 ALP = 0.600 CA = 0.390
+ EXP M = 0.730 ALP = 0.600 CA = 0.393 CW =0.0066

Fig. 9 : VFW VA-2 Airfoil
Calculation with Curvature Effects

shows the good agreement between the present method and the measurements.

The next few figures will show some results from calculations of the flow field around multielement airfoils. Since the effective angle of attack of the model in the tests was uncertain, a suggested increment in Ref. [21] of $\Delta\alpha = -1.0°$ due to the wind tunnel wall correction is chosen. The effective angle of attack quoted in the figures includes this increment.

The first results are for the SKF 1.1 airfoil with extended flap. The solution shown includes the effect of the wake. Fig. 10 shows the pressure distribution at a free stream Mach number of .6 together with the airfoil in the streamline plane. The agreement between the present method and the measurement [21] is good. However, the airfoil contour is not smoothed at the cutout on the main airfoil at the trailing edge.

The same calculation is done but with a free stream Mach number of .7 which produce a greater supersonic region on the airfoil. Fig. 11 shows the result of the present

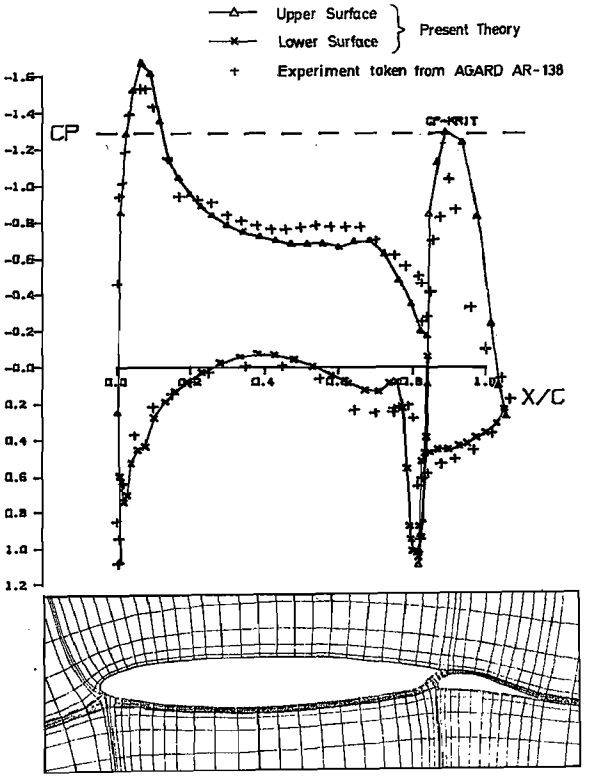

RE = 2.01 MILLION

– THEORY M = 0.600 ALP = 2.000 CA = 1.053
+ EXP M = 0.600 ALP = 3.000 CA = 1.064 CW =0.0139

Fig. 10 : SKF 1.1 Airfoil with Flap
Calculation with Curvature Effects

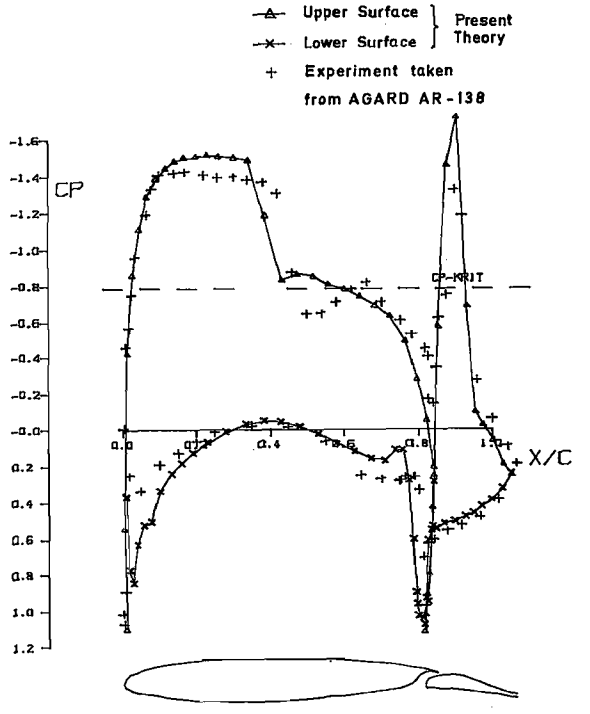

RE = 2.22 MILLION

– THEORY M = 0.700 ALP = 2.000 CA = 1.281
+ EXP M = 0.701 ALP = 3.000 CA = 1.181

Fig. 11 : SKF 1.1 Airfoil with Flap

theory together with measurements of Ref. [21] . The overall agreement is good but the local discrepancis in the shock strength and at the leading edge are probably due to the fact that the pressure distribution in the cut out region of the main airfoil is not well predicted.

A last example is depicted in Fig. 12. It shows the

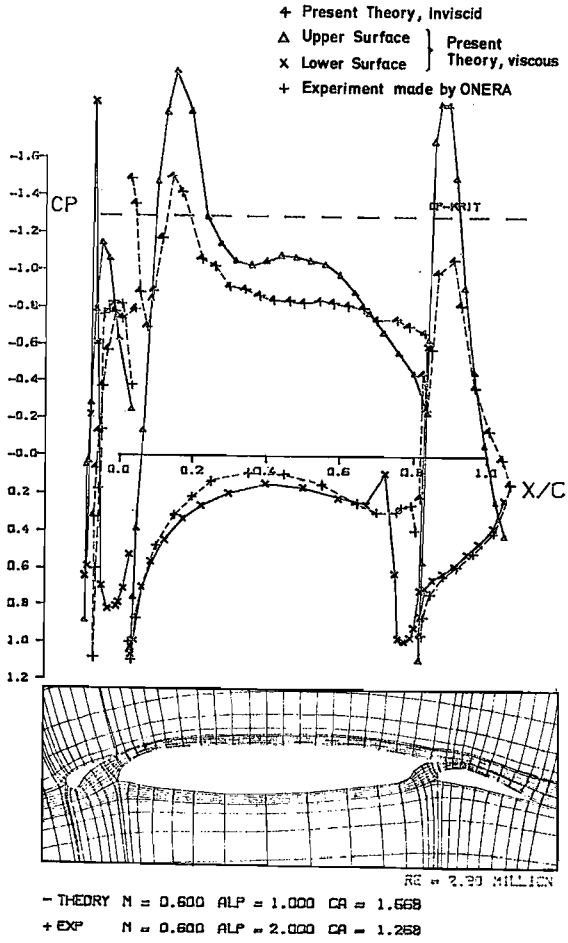

Fig.12: SKF-Conf. C Airfoil with Slat and Flap Comparison with Inviscid Calculation and Measurement

three-element airfoil with slat and flap. Comparison are made with unpublished material of VFW [22] . The agreement between the present theory and the measurement is satisfactory. Note that this prediction is made without wake effects.

The main reason is as follows:

In the interaction region of the gap between main airfoil and flap the boundary layer flow will seperate at the beginning of the cut out. The boundary layer theory are only valid just prior to the seperation point. This leads to a somewhat heuristic seperation streamline based on emperisn and experience. This might be an acceptable way to calculate the boundary layer if only a small seperation region exists. But if massive seperation will appear which is assumed due to the strong adverse pressure gradient like the one shown in the foregoing figures one of the followings have to be done:

To avoid these pressure gradients the airfoil has to be smoothed like a seperation streamline or

the full Navier-Stokes-Equations have to be solved or

to take the results as they are.

If the results are taken as they are no one expects that by using the Kutta-condition, i.e. same velocities on the upper and lower surface at the trailing edge, will give the right circulation. These conditions will lead to the pressure distributuins shown here.

However, the oberall agreement between the present theory and the experiments for single airfoils or even multi-element airfoils are quite satisfactory. For the three-element airfoil the agreement is not as good due to the reason stated above. But for engineering application the results are quite encouraging, since there is little known about the interaction of inviscid/viscous flow around multi-element airfoils in the transonic speed regime.

VI. Conclusions

The method presented here represents a great improvement on those that have been available previously for single or two-element airfoils and has the extension to handle more than two-element airfoil sections. Thus it is of considerable practical value in airfoil design. However, there are deficiencies in the method notable in the region where the boundary layer assumptions are strictly invalid, i.e. when the flow is approaching, or beyond, seperation.

The use of a streamline coordinate transformation procedure in transonic flow analysis allows a general method to be developed that is not confined to a special class of geometry. The method gives results which are in reasonable agreement with experiments. The resulting computer program which has been developed enables a converged solution to be obtained in about 2-3 minutes on an IBM 3033 computer.

VII. References

[1] C.M. Albone, D. Catherall, M.G. Hall, G. Joyce:
An improved numerical method for solving the transonic small pertubation equations for flow past a lifting aerofoil
RAE Technical Report 74056 (1974)

[2] L.A. Carlson:
Transonic Airfoil Analysis and Design Using Cartesian Coordinates
J.Aircraft, Vol 13, No.5, May 1976, pp 349-356

[3] P.C. Bavitz:
An Analysis Method for two-Dimensional Transonic Viscous Flow
NASA TN D-7718, 1975

[4] F. Bauer, P. Garabedian, D. Korn, A. Jameson:
Supercritical Wing Section II
Lecture Notes in Economics and Mathematical Systems, Vol. 108, Springer-Verlag, Berlin, Heidelberg, New York, 1975

[5] K.D. Klevenhusen, R. Hilbig:
Beitrag zur Unterstützung der überkritischen Profilströmung
DGLR-Vortrag Nr. 74-99 (1974)

[6] R.E. Melnik, R. Chow, H.R. Mead:
Theory of Viscous Transonic Flow over Airfoils at High Reynolds Number
AIAA-paper 77-680, 15.th Aerospace Science Meeting Jan.,24-26. 1977, Los Angeles, Calif., USA

[7] M.R. Collyer, R.C. Lock:
Prediction of Viscous Effects in Steady Transonic Flow Past an Aerofoil
Aeronautic. Quart., Aug. 1979, p. 485

[8] C.C.L. Sells:
Plane Subcritical Flow Past a Lifting Aerofoil
Proc. Roy. Soc. (London), Vol 308A, 1968, pp 377-401

[9] J.L. Colehour:
Transonic Flow Analysis Using a Streamline Cootdinate Transformation Procedure,
AIAA-paper 73-657, 6th Fluid and Plasma Dyn. Conf., July 16-18, 1973, Palm Springs, Calif., USA

[10] P. Thiede, G. Dargel:
Hinterkantenströmungen
Verbesserte Erfassung der Reibungseffekte im Hinterkantenbereich von überkritischen Profilen.
RüFo Endbericht T/RF41/70022/71421
VFW-Fokker, 1979

[11] A. Walz:
Boundary Layer of Flow and Temperature, MIT Pres, Cambridge, Massachissetts, (1969)

[12] R.C. Lock:
Calculations of viscous effects on aerofoils in compressible flow.
5th Australian Conference on Hydraulics and Fluid Mechanics, University of Canterbury, N.Z., Dez. 1974

[13] J.L. Hess, A.MO. Smith:
Calculation of Potential Flow About Arbitrary Bodies,
Progress in Aeron. Science, Vol 8, New York, Pergamon Press, 1966

[14] H.J. Oellers:
Die kompressible Potentialströmung in der ebenen Gitterstufe,
WGLR-Jahrbuch, 1962, Braunschweig 1963, p. 349

[15] K.D. Klevenhusen:
A Calculation Method for Multielement Airfoils in Subsonic and Transonic Potential Flow
AIAA-Paper 80-0340, 18.th Aerospace Science Meeting, Jan, 14-16. 1980, Pasadena, Calif. USA

[16] E.M. Murman, J.D. Cole:
Calculation of Plane Steady Transonic Flows.
AIAA-Paper 70-188. 1970

[17] B.C. Arlinger:
Private Communication, 1978

[18] B.C. Arlinger:
Analysis of Two-element High Lift Systems in Transonic Flow,
ICAS-paper 76-13, Oct. 1976

[19] K.P. Burdges, J.A. Blackwell, G.A. Pounds:

High Reynolds Number Test of a NACA 65-213, a = 0.5 Airfoil at Transonic Speeds. NASA CR-2499, March 1975

[20] R.D. Boehe:

Transonik-Messungen am VFW-F Profil. ZKP-Bericht, LFK 7511 Flügelsektion, 1976

[21] Experimental Data Base for Computer Program Assessment AGARD-AR-138, 1979

[22] R.D. Boehe:

Windkanalmessungen mit dem 2D-Modell SKF bei der ONERA Unpublished Paper, VFW